ULUSLARARASI 3B YAZICI TEKNOLOJİLERİ
VE DİJİTAL ENDÜSTRİ DERGİSİ

INTERNATIONAL JOURNAL OF 3D PRINTING
TECHNOLOGIES AND DIGITAL INDUSTRY

ISSN:2602-3350 (Online)

URL: https://dergipark.org.tr/ij3dptdi

MECHANICAL EVALUATION OF VORONOI-CORE SANDWICH STRUCTURES BY ADDITIVE MANUFACTURING

Yazarlar (Authors): Emre AKIN*, Murat ŞEN

Bu makaleye şu şekilde atıfta bulunabilirsiniz (To cite to this article): *Akın E., Şen M., "Mechanical Evaluation of Voronoi-Core Sandwich Structures by Additive Manufacturing" Int. J. of 3D Printing Tech. Dig. Ind., 10(1): 59-72, (2026).*

DOI: 10.46519/ij3dptdi.1786985

Araştırma Makale/ Research Article

Erişim Linki: (To link to this article): https://dergipark.org.tr/en/pub/ij3dptdi/archive

MECHANICAL EVALUATION OF VORONOI-CORE SANDWICH STRUCTURES BY ADDITIVE MANUFACTURING

Emre AKIN[a]*, Murat ŞEN[b]

[a]Marmara University, Technology Faculty, Metallurgical and Materials Engineering Department, TÜRKİYE
[b]Marmara University, Technology Faculty, Mechanical Engineering Department, TÜRKİYE

* *Corresponding Author:* emre.akin@marmara.edu.tr

(**Received:** 19.09.25; **Revised:** 29.12.25; **Accepted:** 20.01.26)

ABSTRACT

This study investigates the mechanical behavior of Voronoi-core sandwich structures fabricated from Tough PLA using FDM. The Voronoi texture generated stochastic, organic-like pores resembling natural open-cell materials. Five core configurations (V0.2–V1.0) were designed with varying pore density while maintaining approximately 33-35 wt% material usage relative to the fully solid reference (V0). Low pore-density specimens with thicker and larger surface-area bridges between pores (e.g., V0.2) outperformed high pore-density specimens with thinner, narrower, lower surface-area walls (e.g., V1.0). In compression, V0.2 achieved the highest modulus (62.94 MPa) and stresses of 2.05 MPa (σ10) and 5.71 MPa (σ50), nearly doubling V1.0. Flexural strength decreased with density (14.7 MPa in V0.2 vs. 5.4 MPa in V1.0), while flexural modulus showed an opposite trend, peaking at 141.2 MPa for V0.8. Impact tests confirmed that V0.2 resisted crack initiation up to 9 inches (2036 mJ), initially as surface indentation, whereas V1.0 failed at 6 inches (1357 mJ). At 25 inches, all porous specimens experienced severe damage, though coarser designs showed more progressive failure. Although weaker than solid V0, Voronoi-core sandwiches demonstrated promising mechanical efficiency at ~33-35 wt% material usage, highlighting their potential as bio-inspired cores for lightweight structural applications.

Keywords: Voronoi-core, Sandwich Structures, PLA-based Materials, Additive Manufacturing, Mechanical Properties.

1. INTRODUCTION

Additive manufacturing (AM), often known as 3D printing, refers to a family of processes in which parts are created directly from digital models by depositing material sequentially in thin layers [1-2]. In contrast to traditional formative or subtractive techniques, AM enables the production of complex geometries without relying on molds or extensive machining [3]. Typically, the workflow begins with the design of a component in computer-aided design (CAD) software, which is then converted into a stereolithography (STL) file. This file is further processed by slicing software that divides the model into layers, each containing the path information required for printing. As a result, AM provides a versatile route for producing lightweight structures with intricate internal features [4-5].

Sandwich structures, consisting of thin outer face sheets and lightweight porous or cellular cores, have long been employed in engineering applications where low weight must be combined with mechanical efficiency [5-7]. Their excellent strength-to-weight ratio, flexural stiffness, and energy absorption capacity have led to extensive use in aerospace, marine, automotive, civil, and renewable energy sectors [8-10]. Conventional core designs such as honeycomb, rhombus, and periodic triangular, square, or hexagonal lattices remain widely used because of their predictable and stable geometry [5,11-13]. However, their intrinsic geometric regularity restricts design flexibility and fails to capture the complexity and irregularity of naturally occurring cellular systems.

The literature survey reflects significant progress being reported on the development of advanced core materials for sandwich structures. In this framework, Vigliotti et al. [14] proposed two-dimensional modern hierarchical honeycomb architectures and demonstrated that several hybrid hierarchical configurations can ensure significant enhancement in stiffness and strength. Similarly, Côté et al. [15] designed corrugated core geometries and demonstrated that their shear strength performance was significantly better than state-of-the-art foam cores and diamond lattices, while being comparable to or higher than the square honeycomb cores. Among other relevant contributions, Santos et al. [16] presented egg-box core sandwich panels manufactured using sisal fibers and castor-oil-based polymer matrices, ensuring around a 45% increase in Charpy impact resistance against conventional composite counterparts, with a strong impact energy absorption capability of the egg-shaped sandwich architectures.

Beyond these deterministic and periodically designed core concepts, Voronoi-based architectures represent a fundamentally different approach by providing a stochastic, bio-inspired morphology, strongly resembling cancellous bone and coral skeletons, among other naturally occurring porous networks, which offers increased design freedom, potentially combined with enhanced damage tolerance and energy dissipation. Their irregular yet space-filling geometry introduces variability in pore density, cell wall thickness, and the surface width of the walls between pores. These characteristics may improve load distribution under stress and create opportunities for enhanced compressive, flexural, and impact performance compared to traditional periodic lattices. Nevertheless, despite the increasing integration of additive manufacturing into structural design, Voronoi geometries remain largely underexplored as functional core materials for sandwich panels [17-19].

A crucial factor in such studies is the choice of material. Polylactic acid (PLA) has become one of the most widely used thermoplastics in fused deposition modeling (FDM) owing to its favorable balance of printability, mechanical strength, and sustainability. Unlike acrylonitrile butadiene styrene (ABS), PLA is derived from renewable resources, biodegradable under industrial composting conditions, and does not release harmful emissions during processing. At the same time, it provides sufficient tensile strength, flexural stiffness, and dimensional accuracy to fabricate structural sandwich components with reliable performance. These attributes have positioned PLA not only as a common material in rapid prototyping but also as a promising candidate for sustainable engineering applications ranging from biomedical implants to lightweight load-bearing components [20-23].

In this study, Voronoi-core sandwich specimens were designed in Blender using a Voronoi texture algorithm [17-19] and subsequently fabricated from PLA via FDM 3D printing to evaluate the influence of internal geometry on mechanical response. Five distinct Voronoi configurations (V0.2 to V1.0) were generated, each constrained to approximately 33-35% of the weight of a fully solid control specimen (V0), while systematically varying cell size and geometric cell density. The V0.2 configuration contained large, sparsely distributed pores with thick walls, whereas V1.0 featured a dense network of small pores with thin, closely packed walls. The mechanical performance of these specimens was assessed through compression, three-point flexural, and drop-weight impact testing. This systematic approach enabled the investigation of how pore density, cell wall thickness, and wall surface width influence structural properties. The results consistently demonstrated that lower pore-density structures exhibited higher compressive and flexural strength, greater modulus values, and superior impact absorption capacity compared to denser porous configurations.

When comparing our findings with the existing literature, Faidallah et al. [1] investigated the mechanical behavior of FDM-fabricated PLA sandwich structures with honeycomb and rhombus cores. Their results showed that rhombus cores exhibited superior performance, achieving a flexural strength of ~12 MPa and compressive strength of ~7 MPa, compared to ~7 MPa and ~4 MPa, respectively, for honeycomb cores. In contrast, the Voronoi-core specimens developed in this study reached a flexural strength of 14.7 MPa, surpassing both honeycomb and rhombus configurations, while their compressive strength of 5.7 MPa was

higher than that of honeycomb cores but slightly lower than that of rhombus structures. An additional consideration is relative density: Faidallah et al. [1] reported solid fractions of ~31% for rhombus and ~27% for honeycomb, whereas the Voronoi-core specimens in this work exhibited ~33–35%. This comparison underscores that, even at slightly higher relative densities, Voronoi architectures provide competitive mechanical performance and highlight their potential as tunable alternatives to conventional lattice-based sandwich cores.

The main motivation of this work is therefore twofold: (i) to establish the structure–property relationships in Voronoi-based sandwich structures with ~33–35 wt% solid content, and (ii) to position Voronoi architectures as sustainable and mechanically viable alternatives to conventional porous cores when manufactured with PLA via FDM technology.

2. MATERIAL and METHOD

Tough PLA (Polylactic Acid), are widely used in 3D printing due to their reliable performance across a range of applications, with each offering distinct advantages [24-25]. while PLA was chosen for its environmentally friendly, biodegradable nature and its ability to print at low temperatures, making it ideal for prototyping. Tough PLA was purchased from by the manufacturer, Porima 3D and their properties are detailed in Table 1 [23]. The 3D models for Voronoi-core sandwich specimens were designed using Blender 3.4 and converted into STL format to ensure compatibility with the 3D printing process. Experimental test specimens were fabricated using an Elegoo Neptune 4 Pro 3D printer with 100% infill density, a layer height of 0.05 mm and a nozzle diameter of 0.4 mm. Printer-specific settings defined in the Orca Slicer software were applied during manufacturing. For filament settings, the generic presets provided by the software for each material type were used. Nozzle temperatures were set based on the average of the minimum and maximum extrusion temperatures recommended by the manufacturer, while the bed temperature was set to the maximum advised value. All specimens were printed with linear infill patterns on a heated bed without any support structures. Table 2 summarizes the printing process parameters used in this study. Following the printing process, support structures were removed and surface finishing was applied. The parts were then inspected for dimensional accuracy and surface quality. In Blender, the Voronoi texture function, which closely resembles an organic porous structure, was employed to design sandwich models with cores of varying pore characteristics. These models maintained approximately the same overall weight ratios but differed in porosity density, incorporating variations in pore size, distribution, and wall thickness. The compression models designed in Blender are presented in Figure 1. The designs were prepared for both compression and flexural testing. When 3D printed, all porous models exhibited approximately 33-35 wt% of the mass of the fully solid reference cube, with detailed weight ratios provided in Table 3. Based on their porosity density, the porous cores were designated as V1, V0.8, V0.6, V0.4, and V0.2, as listed in Table 3, while the fully solid specimen was coded as V0. The finalized models were processed using Orca Slicer software with a 100% infill density and a layer height of 0.05 mm. Printing was performed on an Elegoo Neptune 4 Pro 3D printer equipped with a 0.4 mm nozzle, under the processing parameters summarized in Table 2.

Table 1. The properties of Tough PLA filaments

Physical Properties	Density (g/cm^3)	1.22
	Melted Flow Index (g/10min)	17.3
Mechanical Properties	Tensile Strength (MPa)	50
	Elastic Modulus (GPa)	2.4
	Elongation at Break (%)	50
	Impact Strenght (kJ/m^2)	36
Thermal Properties	Heat Deflection Temperature (°C)	58
	Transition Temperature (°C)	55-65

Table 2. The printing process parameters for Tough PLA filament

Nozzle Temperature (°C)	265
Bed Temperature (°C)	60
Print Speed (mm/s)	200
Cooling Fan Settings	100% after first layer

Table 3. Weight fraction of solid content of Voronoi-core sandwich specimens

Samples	Weight Fraction of Solid Content (%)
V0.2	34
V0.4	33
V0.6	35
V0.8	34
V1	34

Flexural tests of the Voronoi-core sandwich specimens were performed on a Zwick Z010 universal testing machine at a crosshead speed of 5 mm/min under ambient temperature conditions, in accordance with ISO 178. The analysis focused on ultimate flexural strength, flexural modulus, and elongation at break. Compressive tests of the Voronoi-core sandwich specimens were conducted in accordance with the ISO 844 method, also using a Zwick Z010 testing machine at a crosshead speed of 3 mm/min under ambient conditions. Prior to and following compression testing, the pore morphology, distribution, and wall characteristics of the cores were examined using a Carl Zeiss Ultra Plus scanning electron microscope (SEM) operated at an acceleration voltage of 20 kV. For SEM analysis, the specimens were sputter-coated with a 2–4 nm layer of Au/Pd using a Quorum Q150R ion beam sputtering system.

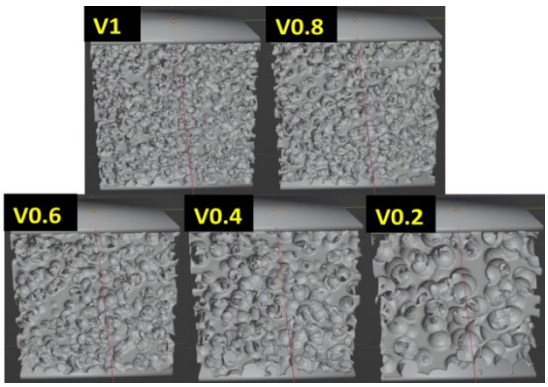

Figure 1. 3D-rendered Voronoi-core sandwich structures with graded cell size and density

The impact resistance of the Voronoi-core sandwich structures was evaluated using a Sheen tubular impact (drop) tester equipped with a 908 g steel ball of 16.3 mm diameter and a 25-inch drop tube with a weight-locking collar, in accordance with ASTM D7136. The potential energy of the impact was correlated with the damage mechanisms observed on the porous plates, including crack initiation, crack propagation, surface indentation, dome-shaped deformation, fragmentation, delamination, back-face damage, and core compression. Drop heights up to 25 inches were applied during testing. The experimental setup of the Sheen impact drop test is shown in Figure 2, while Figure 3 presents the 3D-printed specimens prepared for both compression and Sheen impact tests. For the Sheen impact test, the sandwich plates were fabricated with dimensions of 50 × 50 × 10 mm.

For each sample type (code), five specimens were prepared, and the reported values correspond to the average of these five results. The coefficient of variation (CoV) was also calculated and presented in the tables and figures. CoV is defined as the ratio of the standard deviation to the mean, multiplied by 100, as expressed in Equation (1)

$$\mathrm{CoV} = \frac{s}{\mu} x100 \qquad (1)$$

where s is the standard deviation and μ is the mean value.

CoV represents a measure of relative variability and is commonly used to compare the degree of dispersion across different datasets. In addition to assessing relative risk, it can also serve to indicate the likelihood or probability distribution of the results. While the standard deviation describes the absolute spread of values around the mean, CoV normalizes this spread by the mean, thus providing a dimensionless indicator of variability.

Figure 2. Experimental setup of the Sheen impact drop test used for evaluating impact resistance of Voronoi-core sandwich specimens

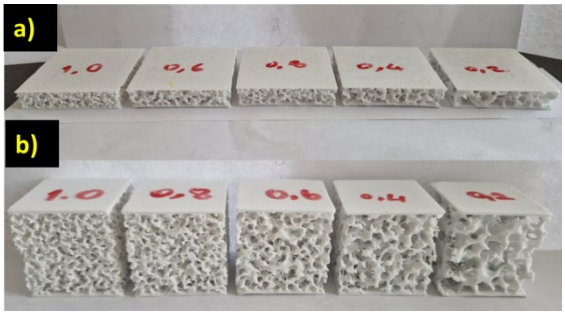

Figure 3. Voronoi-core sandwich specimens prepared for mechanical testing: a) specimens before impact test, b) specimens before compression test

3. RESULTS and DISCUSSION

The compressive properties of the Voronoi-core sandwich specimens revealed an inverse relationship between geometric cell density and mechanical performance. As the cell size decreased and the number of cells per unit area increased, both compressive stiffness and strength were observed to decline. The V0.2 specimen, which possessed the largest cell size and lowest cell density, exhibited the highest compressive modulus at 62.94 MPa. By contrast, the V1 configuration, which contained the smallest and most densely arranged cells, yielded a compressive modulus of just 33.4 MPa. This trend was also evident in the compressive stress values: at 10% strain, stress decreased from 2.05 MPa in V0.2 to 1.23 MPa in V1.0, and at 50% strain, from 5.71 MPa to 4.42 MPa, respectively.

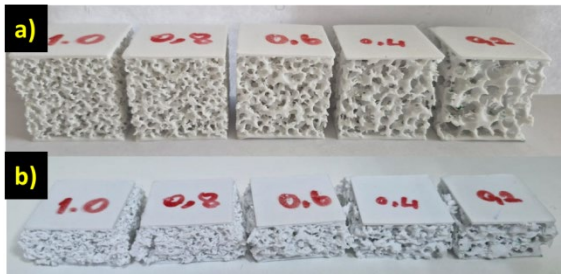

Figure 4. Voronoi-core sandwich specimens prepared for compression testing: a) specimens before compression test, b) specimens after compression test

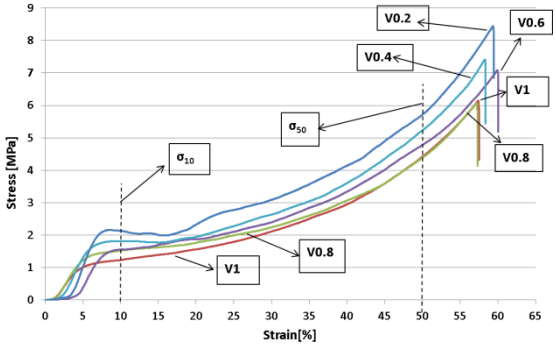

Figure 5. Compressive stress–strain curves of Voronoi-core sandwich specimens (V0.2–V1.0) with indication of stress values at 10% and 50% strain

Table 4. Compression test values of Voronoi-core sandwich specimens

Samples	σ_{10} (MPa)	CoV	σ_{50} (MPa)	CoV	Modulus (MPa)	CoV
V0	Test not able to be performed due to exceeding the 1-ton load capacity of the machine					
V0.2	2.05± 0.06	3.16	5.7± 0.12	2.19	63.02± 1.69	2.68
V0.4	1.80± 0.03	1.82	5.2± 0.07	1.47	49.75± 1.76	3.54
V0.6	1.64± 0.03	2.08	4.7± 0.05	1.07	41.34± 1.55	3.77
V0.8	1.53± 0.02	1.69	4.3± 0.04	1.02	39.57± 1.18	3
V1	1.24± 0.02	2.09	4.4± 0.03	0.86	33.44± 1.16	3.49

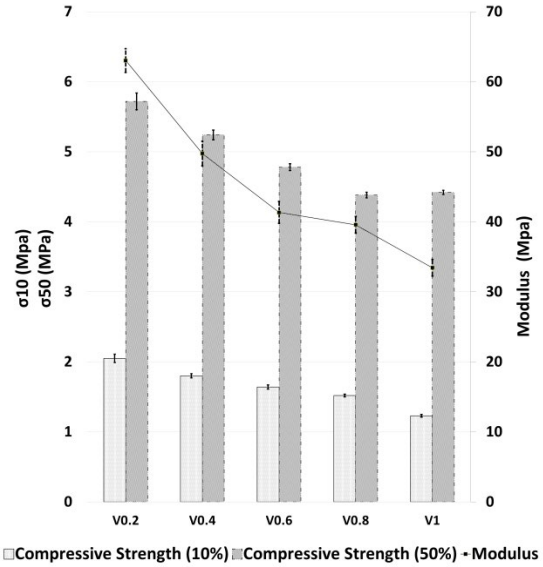

Figure 6. Compressive properties of Voronoi-core sandwich specimens

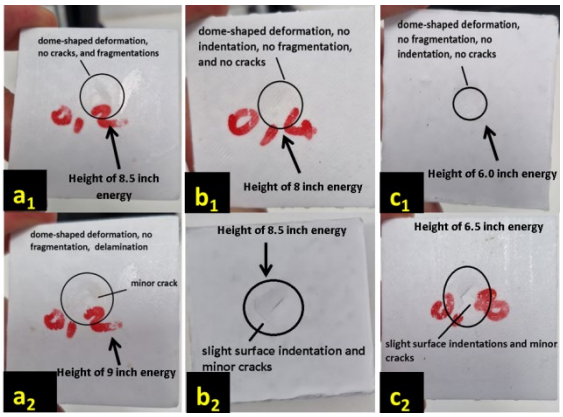

Figure 7. Impact damage morphology of foam specimens at varying drop heights, where subscripts 1 and 2 indicate the last no-crack deformation and the first crack-initiation height, respectively: a) V0.2, b) V0.4, and c) V0.8.

This behavior suggests that the thinner and narrower cell walls at the interconnections of highly dense Voronoi structures are more susceptible to local instability, leading to premature failure through buckling or stress concentration. In contrast, architectures characterized by larger pores and thicker cell walls provide more robust structural bridges, thereby enhancing stiffness and promoting more uniform stress distribution during loading. Consequently, these coarser architectures act as stronger foam-like frameworks capable of sustaining higher loads without localized collapse. Figure 4 illustrates the Voronoi-core sandwich specimens in their initial state prior to compression testing and the deformation modes observed after testing, while the compressive stress–strain curves and values presented in Figure 5 and 6 further substantiate this hypothesis. Moreover, Table 4 shows all compressive values. Taken together, Figures 4 and 5 provide consistent evidence that pore density, cell wall thickness, and the surface width of the walls between pores are critical determinants of the deformation behavior of Voronoi-core structures under compressive loading. V0.2 exhibited a more stable and nearly linear deformation profile, whereas denser configurations such as V0.8 and V1 displayed early softening and nonlinear responses, symptomatic of localized deformation and progressive wall collapse. Moreover, it is notable that all porous specimens exhibited negligible elastic recovery after unloading, indicating an absence of resilience and confirming the predominantly plastic nature of the deformation. Analysis of the quantitative results presented in Figures 7 and 8, clearly demonstrates the advantages of low-density Voronoi structures. At 10% strain (σ10), V0.2 achieved 2.05 MPa, which is approximately 67% higher than V1 (1.23 MPa). At 50% strain (σ50), the difference remained pronounced, with V0.2 reaching 5.71 MPa, which was approximately 29% greater than V1 (4.42 MPa). Similarly, the compressive modulus of V0.2 (62.94 MPa) exceeded that of V1 (33.4 MPa) by nearly 89%, underscoring the decisive role of wall thickness and load-bearing bridges in coarse Voronoi architectures. It is also important to emphasize that while all Voronoi-core configurations exhibited compressive strengths markedly lower than the fully solid reference specimen (V0), the test could not be completed for V0 due to the 1-ton load limitation of the testing apparatus. Nonetheless, within the porous group, the superior compressive and impact performance of low-density Voronoi designs demonstrates that optimizing pore size, wall thickness and surface width is more effective than maximizing cell density alone.

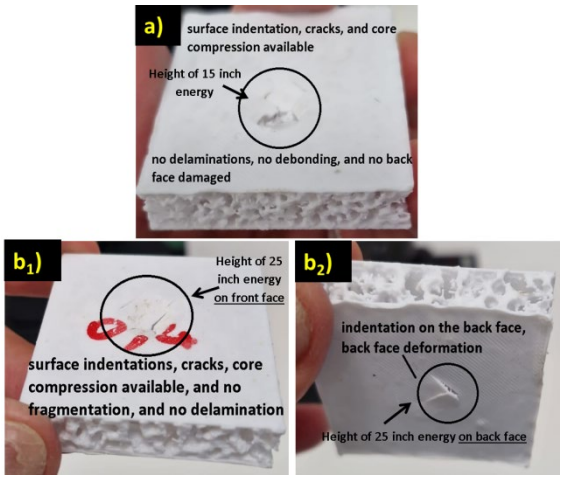

Figure 8. Impact damage morphology of Voronoi-core sandwich specimens after high-energy drop tests: a) V0.8 at 15 inches, b1) V0.4 front face at 25 inches, and b2) V0.4 back face at 25 inches

Impact resistance followed a similar trend to the compressive results. The drop-weight impact tests revealed that crack initiation occurred at higher energy levels in specimens with lower cell density. Specifically, V0.2 withstood an impact energy of 2036 mJ at a 9-inch drop height before the onset of cracking, whereas V1.0 failed at only 6 inches and 1357 mJ. Intermediate configurations (V0.4–V0.8) demonstrated a progressive decline in performance, with crack initiation occurring at 8.5 inches for V0.4, 7 inches for V0.6, and 6.5 inches for V0.8, confirming a gradual decrease in resistance as cell density increased. The visual examinations in Figures 5 and 7 further substantiate this trend. Coarser structures such as V0.2 exhibited only very slight indentation and dome-shaped deformation at lower drop heights (<9 inches), with significant damage only developing at higher energy levels (15–25 inches). By contrast, denser structures (V0.8 and V1.0) displayed earlier crack initiation, less stable deformation modes, and widespread damage propagation even at moderate drop heights (6–7 inches). These results clearly indicate that larger cells, thicker walls, and wider surface widths of the walls between pores promote more effective load distribution, greater deformation capability, and enhanced energy dissipation under high strain-rate impact loading. Despite the differences in impact performance, all specimens consistently exhibited no signs of delamination between the core and the face sheets, underscoring the structural reliability of the monolithically printed sandwich design.

The height measured for each sample was subsequently transformed into potential energy utilizing Equation 1.

$$E = m \times g \times h \quad (1)$$

In this equation, E represents potential energy, m denotes the mass of the steel ball (in kilograms), g signifies gravitational acceleration (about 9.81 m/s²), and h indicates the height from which the weight is released (in meters). Table 5 shows the potential energy corresponding to the height.

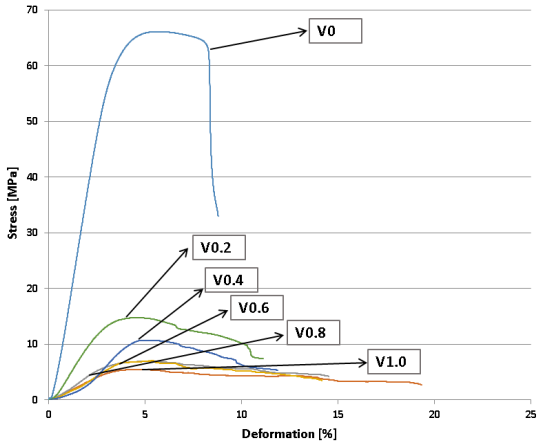

Figure 9. Flexural stress–strain curves of Voronoi-core sandwich specimens

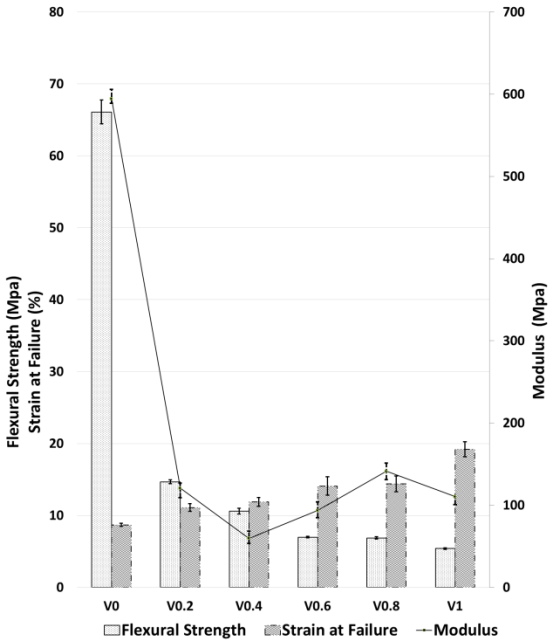

Figure 10. Flexural properties of Voronoi-core sandwich specimens

Taken together, the results confirm that Voronoi-core sandwiches with coarser architectures (e.g., V0.2) deliver superior impact resistance compared with denser designs (e.g., V1.0), and that this advantage arises from the thicker walls and wider structural bridges inherent to low-density Voronoi networks. All impact-related characteristics of the samples are summarized in Table 5.

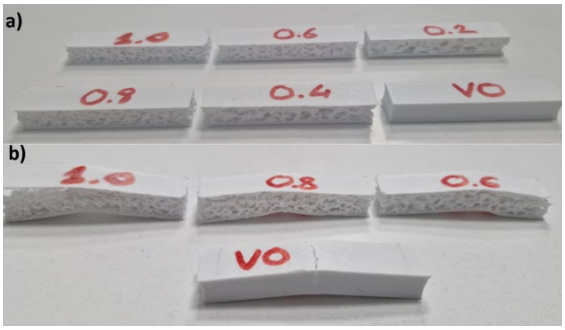

Figure 11. Voronoi-core sandwich specimens prepared for flexural testing: a) specimens before flexural test, b) core shear specimens after flexural test

The flexural behavior of the Voronoi-core sandwich specimens exhibited both parallels and contrasts with the compressive results. As shown in Figure 9 and 10, flexural strength followed the same trend as compression, decreasing consistently with increasing geometric density. Moreover, all flexural values are shown in Table 6. V0.2 displayed the highest flexural strength (14.7 MPa), which was 37% greater than V0.4 (10.7 MPa) and nearly 172% higher than V1.0 (5.4 MPa). This confirms that specimens with larger cells, thicker walls, and wider surface connections between pores can withstand higher bending stresses before failure. However, the variation in flexural modulus diverged from the compressive modulus trend. While V0.2 and V0.4 exhibited relatively low moduli (120.8 MPa and 59.9 MPa, respectively), the values increased from V0.6 (93.4 MPa) onward, reaching a peak of 141.2 MPa in V0.8 before decreasing slightly in V1.0 (110.2 MPa). This indicates that the structural bridges formed by thinner but more numerous cell walls in denser designs contribute differently under bending, providing increased stiffness despite their lower flexural strength. Deformation modes observed in Figure 11 corroborate these findings. In the denser specimens (V0.6, V0.8, and V1.0), core shear deformation was the predominant failure mechanism, reflecting the relative contribution of the interconnected thin walls to resisting bending-induced shear stresses. By contrast, in the coarser structures (V0.2 and V0.4), face sheet buckling and localized crushing dominated, highlighting that the thicker cell walls and the wider surface width of the walls between pores resisted shear but transferred stresses to the face sheets, leading to instability under flexural loading.

Similar deformation modes, particularly core shear and local indentation, are commonly observed in sandwich panels subjected to three-point bending tests. These mechanisms were likewise reported by Mamalis et al. [27]. These results suggest that while the superior wall thickness of coarse Voronoi designs enhances flexural strength, the higher wall connectivity in denser designs can locally increase flexural modulus by redistributing shear stresses across a larger number of thinner bridges. The combination of these competing effects underscores that pore size, wall thickness, and bridge density do not affect compressive and flexural properties identically, but instead interact differently depending on the mode of loading.

Overall, the superior compressive, flexural, and impact absorption properties observed in low pore-density Voronoi-core sandwich specimens can be attributed to the thicker cell walls and the wider surface width of the walls between pores. As clearly visible in Figure 1, these geometric features are more pronounced in the coarser Voronoi architectures designed in Blender, forming more stable load-bearing bridges across the structure. This configuration facilitates improved stress distribution; delays crack initiation, and enhance resistance to progressive wall collapse. These findings confirm that the geometry of the pore walls, rather than pore density alone, plays a decisive role in governing the mechanical efficiency of Voronoi-core sandwich structures. In the literature, relatively few studies have examined the application of Voronoi lattices as core materials in sandwich structures.

Table 5. Impact properties of Voronoi-core sandwich specimens

Samples	Drop height (inch)	Corresponding potential energy (E, mj)	Crack initiation Observed	Cracking level	Surface indentation	Dome-shaped deformation	Fragmentation	Delamination	Back face damage	Core compression
V0	25	5659	no	-	no	no	no	no	no	no
V0.2	<5	<1130	no	-	no	no	no	no	no	no
V0.2	5	1130	no	-	very slight	very slight	no	no	no	no
V0.2	8.5	1921	no	-	very slight	very slight	no	no	no	no
V0.2	9	2034	yes	very slight	very slight	very slight	no	no	no	no
V0.2	15	3393	yes	major	major	major	no	no	major	major
V0.2	25	5659	yes	major	major	major	no	no	major	major
V0.4	<5	1130	no	-	no	no	no	no	no	no
V0.4	5	<1130	no	-	very slight	very slight	no	no	no	no
V0.4	8.0	1809	no	-	slight	slight	no	no	no	no
V0.4	8.5	1921	yes	slight	slight	slight	no	no	no	no
V0.4	15	3393	yes	major	major	major	no	no	major	major
V0.4	25	5659	yes	major	major	major	no	no	major	major
V0.6	<5	<1130	no	-	no	no	no	no	no	no

V0.6	5	1130	no	-	very slight	very slight	no	no	no	no
V0.6	6.5	1471	no	-	slight	slight	no	no	no	no
V0.6	7	1583	yes	slight	slight	slight	no	no	no	no
V0.6	15	3393	yes	major	major	major	no	no	major	major
V0.6	25	5659	yes	major	major	major	no	no	major	major
V0.8	<5	<1130	no	-	no	no	no	no	no	no
V0.8	5	1130	no	-	very slight	very slight	no	no	no	no
V0.8	6.0	1360	no	-	slight	slight	no	no	no	no
V0.8	6.5	1471	yes	slight	slight	slight	no	no	no	no
V0.8	15	3393	yes	major	major	major	no	no	major	major
V0.8	25	5659	yes	major	major	major	no	no	major	major
V1	<5	<1130	no	-	no	no	no	no	no	no
V1	5	1130	no	-	very slight	very slight	no	no	no	no
V1	5.5	1246	no	-	very slight	very slight	no	no	no	no
V1	6	1360	yes	very slight	very slight	very slight	no	no	no	no
V1	15	3393	yes	major	major	major	no	no	major	major
V1	25	5659	yes	major	major	major	no	no	major	major

Table 6. Flexural test values of Voronoi-core sandwich specimens

Samples	σ_f (MPa)	CoV	E_f (MPa)	CoV	ε_m (%)	CoV
V0	66.1 ±1.67	2.52	594.4± 5.23	0.88	8.76± 0.21	2.37
V0.2	14.7 ±0.28	1.92	120.6± 11.27	9.34	11.14± 0.53	4.78
V0.4	10.6 ±0.41	3.88	59.78± 6.29	10.53	11.96± 0.62	5.17
V0.6	7.0± 0.10	1.41	93.64± 8.91	9.51	14.10± 1.26	8.94
V0.8	6.89 ±0.16	2.35	141.3± 10.27	7.27	14.44± 1.09	7.53
V1	5.41 ±0.11	2.01	110.3± 9.74	8.83	19.28± 1.03	5.33

* σ_f: flexural strength
* E_f: flexural modulus
* ε_m: elongation at break

Gür et al. [28] fabricated 3D-printed Voronoi lattice core sandwich composites with woven glass fiber–epoxy face sheets and compared them with counterparts incorporating rectangular prism cores. Their results demonstrated that the three-point bending properties of the Voronoi-core sandwich structures were superior to those of the rectangular prism designs. Similarly, Faidallah et al. [1] investigated PLA-based sandwich structures produced via FDM using rhombus and honeycomb cores. When benchmarked against their reported performance, the PLA-based Voronoi-core sandwich specimens developed in the present study exhibited markedly enhanced strength characteristics. Moreover, beyond their advantages in strength, toughness, and impact resistance, the adoption of PLA, owing to its biodegradability and sustainability, further underscores the novelty and broader relevance of the present work [29].

Accordingly, open-cell Voronoi structures of various cell densities were designed using Blender by changing the number of nuclei, but keeping the overall weight of the specimens nearly constant. The structure with the highest cell density was denoted V1, and that with the lowest cell density was denoted V0.2. In this approach, the number of nuclei of V1 was defined as 100%, while that for V0.2 corresponded to 20% of this maximum value.
It should be pointed out that with the increase in Voronoi cell density, a reduction in strut thickness and strut surface area is evidenced quite clearly. This was realized both in the printed specimens and in the morphological features of the Voronoi models created in Blender. In flexural and compressive testing of PLA-based foam structures, their deformation took place primarily through strut collapse and interfacial failure between adjacent layers.

Wang et al. [30] also report similar behavior for PLA-based open-cell Voronoi structures. Increasing the strut thickness in their study increased the relative density and significantly improved both compressive stress and elastic modulus. The strut diameter was varied from 0.7 mm up to 1.2 mm and significantly improved the compressive properties of the structures. PLA Voronoi specimens were further compared with PA-based Voronoi structures fabricated from PA6 and PA12. PLA specimens exhibited negligible or no recovery after compression, while the PA6 and PA12 specimens showed a quite distinct recovery from their compacted states. This PLA behavior is shown in Fig. 4(b) of the present study. Such behavior was linked to the governing modes of deformation dominated by strut collapse and debonding at the relatively weak interlayer interfaces in PLA structures.

These results indicate that even when the Voronoi architecture is similar, different polymer materials may exhibit different deformation mechanisms under mechanical loading. Another work focusing on metallic Voronoi-cell structures reported that cell regularity exerted a stronger effect on mechanical behavior than cell size or cell density did [31]. Overall, the Voronoi-based cellular structures represent a relatively new research area in additive manufacturing. The results show that there is still great potential for further studies, especially regarding how material type, cell density, and deformation mechanisms may influence mechanical properties.

4. CONCLUSION

This study demonstrated that Voronoi-textured sandwich structures with 33-35% solid content exhibit mechanical trends strongly governed by pore density, cell wall thickness, and the surface width of the walls between pores. Low pore-density specimens with thicker walls and broader surface widths between pores (e.g., V0.2) consistently outperformed high pore-density designs with thinner walls and narrower surface widths (e.g., V1.0) in terms of compressive stiffness, strength, and impact resistance. Specifically, V0.2 achieved a compressive modulus of 62.94 MPa and stresses of 2.05 MPa (σ10) and 5.71 MPa (σ50), nearly doubling the performance of V1.0. In flexural loading, strength declined with increasing pore density (14.7 MPa in V0.2 vs. 5.4 MPa in V1.0), whereas the flexural modulus rose with denser configurations (from 93.4 MPa at V0.6 to 141.2 MPa at V0.8), reflecting the distinct contribution of thinner but more numerous walls under bending. Impact tests further highlighted these contrasts: in V0.2, crack initiation was delayed to 9 inches (2036 mJ) and appeared initially only as superficial indentation, while V1.0 failed at 6 inches (1357 mJ). At the highest potential energy level (25 inches), all specimens experienced severe damage including core compression, though the failure progression was more stable in coarse designs. While the Voronoi-core panels exhibited lower mechanical properties than the fully solid reference (V0), their efficiency at 33-35% material usage demonstrates the viability of Voronoi architectures for lightweight sandwich applications. Future research should focus on optimizing hybrid or graded Voronoi structures, exploring higher-performance polymers, and refining wall connectivity to balance compressive, flexural, and impact properties for demanding structural applications.

REFERENCES

1. Faidallah, R. F., Hanon, M. M., Szakál, Z., and Oldal, I., “Study of the mechanical characteristics of sandwich structures FDM 3D-printed”, Acta Polytechnica Hungarica, Vol. 20, Issue 6, Pages 7–23, 2023.

2. Keşkekçi, A. B., Özkahraman, M., and Bayrakçı, H. C., “A review on the impact of polylactic acid (PLA) material on products manufactured using fused deposition modeling (FDM) additive manufacturing method”, Gazi Journal of Engineering Sciences, Vol. 9, Issue 4, Pages 158–173, 2023.

3. Aydın, N., “A new bio-inspired wing design with 3D additive manufacturing scanning and printing method: MJF technology”, Eskişehir Technical University Journal of Science and Technology A- Applied Sciences and Engineering, Vol. 24, Issue 4, Pages 250–256, 2023.

4. Çakır, M., and Akın, E., “Nanocomposites obtained from various acrylate resins with DPGDA reactive diluent filled with fumed silica particles produced by using a DLP/LCD-type 3D printer”, Journal of Innovative Engineering and Natural Science, Vol. 4, Issue 2, Pages 672–683, 2024.

5. Sahu, S. K., Sreekanth, P. S. R., and Reddy, S. V. K., “A brief review on advanced sandwich structures with customized design core and composite face sheet”, Polymers, Vol. 14, Issue 20, Pages 4267, 2022.

6. Kolodziejska, J. A., Roper, C. S., Yang, S. S., Carter, W. B., and Jacobsen, A. J., “Research update: Enabling ultra-thin lightweight structures: Microsandwich structures with microlattice cores”, APL Materials, Vol. 3, Issue 5, Pages 050701, 2015.

7. Xiong, J., Du, Y., Mousanezhad, D., Eydani Asl, M., Norato, J., and Vaziri, A., “Sandwich structures with prismatic and foam cores: A review”, Advanced Engineering Materials, Vol. 21, Issue 1, Pages 1800036, 2019.

8. Kamble, Z., “Advanced structural and multi-functional sandwich composites with prismatic and foam cores: A review”, Polymer Composites, Vol. 45, Issue 18, Pages 16355–16382, 2024.

9. Patekar, V., and Kale, K., "State of the art review on mechanical properties of sandwich composite structures", Polymer Composites, Vol. 43, Issue 9, Pages 5820–5830, 2022.

10. Tarlochan, F., "Sandwich structures for energy absorption applications: A review", Materials, Vol. 14, Issue 16, Pages 4731, 2021.

11. Çakır, M., and Akın, E., "Mechanical properties of low-density heat-resistant polyimide-based advanced composite sandwich panels", Polymer Composites, Vol. 43, Issue 2, Pages 827–847, 2022.

12. Araújo, H., Leite, M., Ribeiro, A. M. R., Deus, A. M., Reis, L., and Vaz, M. F., "Investigating the contribution of geometry on the failure of cellular core structures obtained by additive manufacturing", Frattura ed Integrità Strutturale, Vol. 49, Pages 478–486, 2019.

13. Mukherjee, S., Scarpa, F., and Gopalakrishnan, S., "Phononic band gap design in honeycomb lattice with combinations of auxetic and conventional core", Smart Materials and Structures, Vol. 25, Issue 5, Pages 054011, 2016.

14. Vigliotti, A., & Pasini, D., Mechanical properties of hierarchical lattices. Mechanics of Materials, Vol. 62, Pages 32–43, 2013.

15. Côté, F., Deshpande, V. S., Fleck, N. A., & Evans, A. G. The compressive and shear responses of corrugated and diamond lattice materials. International Journal of Solids and Structures, Vol. 43, Pages 6220–6242, 2006.

16. Dos Santos, J. C., da Silva, R. J., Christoforo, A. L., Freire, R. T. S., Tarpani, J. R., Scarpa, F., & Panzera, T. H. Impact performance of egg-box core sandwich panels made from sisal fibers and castor-oil-based polymer. Polymer Composites, Vol. 46, Issue 6, Pages 4958-4966, 2024.

17. Wang, G., Shen, L., Zhao, J., Liang, H., Xie, D., Tian, Z., and Wang, C., "Design and compressive behavior of controllable irregular porous scaffolds: Based on Voronoi-Tessellation and for additive manufacturing", ACS Biomaterials Science and Engineering, Vol. 4, Issue 2, Pages 719–727, 2018.

18. Colamartino, I., Anghileri, M., and Boniardi, M., "Investigation of the compressive properties of three-dimensional Voronoi reticula", International Journal of Solids and Structures, Vol. 284, Pages 112501, 2023.

19. Tee, Y. L., Nguyen-Xuan, H., and Tran, P., "Flexural properties of porcupine quill-inspired sandwich panels", Bioinspiration & Biomimetics, Vol. 18, Issue 4, Pages 046004, 2023.

20. Bardot, M., and Schulz, M. D., "Biodegradable poly(lactic acid) nanocomposites for fused deposition modeling 3D printing", Nanomaterials, Vol. 10, Issue 12, Pages 2567, 2020.

21. Özsoy, K., Erçetin, A., and Çevik, Z. A., "Comparison of mechanical properties of PLA and ABS based structures produced by fused deposition modelling additive manufacturing", European Journal of Science and Technology, Vol. 27, Pages 802–809, 2021.

22. "Strength and dimension accuracy in fused deposition modeling: A comparative study on parts making using ABS and PLA polymers", Jurnal Rekayasa Mesin, Vol. 11, Issue 1, Pages 69–76, 2020.

23. Sandanamsamy, L., Harun, W. S. W., Ishak, I., and others, "A comprehensive review on fused deposition modelling of polylactic acid", Progress in Additive Manufacturing, Vol. 8, Pages 775–799, 2023.

24. All3DP, "3D printing materials guide", Online Resource, August 1, 2025. Retrieved from https://all3dp.com/1/3d-printing-materials-guide-3d-printer-material/

25. Dey, A., Roan Eagle, I. N., and Yodo, N., "A review on filament materials for fused filament fabrication", Journal of Manufacturing and Materials Processing, Vol. 5, Issue 3, Pages 69, 2021.

26. Porima 3D, "3D yazıcı filamentleri", Online Resource, August 5, 2025. Retrieved from https://porima3d.com/

27. Mamalis, A. G., Spentzas, K. N., Manolakos, D. E., Ioannidis, M. B., and Papapostolou, D. P., "Experimental investigation of the collapse modes and the main crushing characteristics of composite sandwich panels subjected to flexural loading", International Journal of Crashworthiness, Vol. 13, Issue 4, Pages 349–362, 2008.

28. Gür, Y., Benlikaya, R., and Çelik, S., "An investigation from raw components to composite: 3D printed Voronoi lattice core structured sandwich composite with woven glass fiber-epoxy outer layer", Engineering Research Express, Vol. 7, Issue 1, Pages 015522, 2025.

29. Saniei, H., and Mousavi, S., "Surface modification of PLA 3D-printed implants by electrospinning with enhanced bioactivity and cell affinity", Polymer, Vol. 196, Pages 122467, 2020.

30. Wang, S., Ding, Y., Yu, F., Zheng, Z., & Wang, Y. Crushing behavior and deformation mechanism of additively manufactured Voronoi-based random open-cell polymer foams. Materials Today Communications, Vol. 25, Pages 101406, 2020.

31. Tang, L., Shi, X., Zhang, L., Liu, Z., Jiang, Z., & Liu, Y. Effects of statistics of cell size and shape irregularity on mechanical properties of 2D and 3D Voronoi foams. Acta Mechanica, Vol. 225, Pages 1361–1372, 2014.